

Complete Hierarchies for the Geometric Measure of Entanglement

Lisa T. Weinbrenner,¹ Albert Rico,² Kenneth Goodenough,¹ Xiao-Dong Yu,³ and Otfried Ghne¹

¹*Naturwissenschaftlich-Technische Fakultt, Universitt Siegen, Walter-Flex-Strae 3, 57068 Siegen, Germany*

²*GIQ - Quantum Information Group, Department of Physics, Autonomous University of Barcelona, Spain*

³*Department of Physics, Shandong University, Jinan 250100, China*

(Dated: February 2, 2026)

In quantum physics, multiparticle systems are described by quantum states acting on tensor products of Hilbert spaces. This product structure leads to the distinction between product states and entangled states; moreover, one can quantify entanglement by considering the distance of a quantum state to the set of product states. The underlying optimization problem occurs frequently in physics and beyond, for instance in the computation of the injective tensor norm in multilinear algebra. Here, we introduce a method to determine the maximal overlap of a pure multiparticle quantum state with product states based on considering several copies of the pure state. This leads to three types of hierarchical approximations to the problem, all of which we prove to converge to the actual value. Besides allowing for the computation of the geometric measure of entanglement, our results can be used to tackle optimizations over stochastic local transformations, to find entanglement witnesses for weakly entangled bipartite states, and to design strong separability tests for mixed multiparticle states. Finally, our approach sheds light on the complexity of separability tests.

I. INTRODUCTION

Entanglement is one of the most studied resources in quantum information theory, being useful for quantum metrology, quantum cryptography or quantum communication [1, 2]. As such, there are numerous ways to characterize and quantify entanglement from different viewpoints. Especially for bipartite pure states the problem of quantifying entanglement is well understood. However, for most practical applications multiparticle states are needed, calling for a better understanding of multiparticle entanglement quantification.

One possible measure of entanglement for quantum states is given by the geometric measure of entanglement, which quantifies the entanglement of a state by its geometric distance to separable states [3–6]. For a pure three-particle state $|\psi\rangle$ it is defined as $E_G(\psi) = 1 - \Lambda^2(\psi)$, where

$$\Lambda^2(\psi) = \max_{|abc\rangle} |\langle abc|\psi\rangle|^2 \quad (1)$$

denotes the maximal overlap between the three-partite $|\psi\rangle$ and all product states $|abc\rangle$. Interestingly, this measure is directly related to different notions considered in mathematics like the injective tensor norm and tensor eigenvalues [7, 8]. For bipartite pure states the measure can be directly evaluated by the Schmidt decomposition; moreover, there are results for special families of multiparticle states [6]. However, the calculation of the geometric measure is known to be computationally difficult for general multipartite states [9], implying a similar statement for the injective tensor norm.

There are several examples of hard optimization problems which can be tackled with so-called hierarchies, forming an infinite sequence of approximations indexed by the level k . Larger k yield tighter bounds, at the cost of increased computational complexity. A hierarchy is complete if, informally speaking, the approximations con-

verge to the actual solution as k tends to infinity. Some notable examples in quantum physics include hierarchies for the separability problem [10], the marginal problem [11], and the question whether or not observed correlations can originate from quantum mechanics [12], and in mathematics the optimization of multivariate polynomials [13].

In this paper we describe three different hierarchies for the geometric measure of pure states which are provably complete. All three hierarchies rely on a multi-copy approach, where given operators act on multiple copies of the target state, leading to increasingly better bounds with the number of copies considered. We illustrate numerically the convergence behavior of the hierarchies for some three- and five-qubit states. Furthermore, we show how the results can be adapted for witness constructions and checking distillability, and use our approach to characterize entanglement in mixed states. Interestingly, one of the hierarchies is closely related to so-called product tests for entanglement [9, 14–16], leading to a natural improvement of this test to more copies. From a mathematical perspective, our work advances a discussion started by Harald A. Helfgott [17], when looking to generalize a well known upper bound on the injective norm (or the largest eigenvalue) of real symmetric matrices to general real symmetric tensors. This was taken up by Shmuel Friedland by introducing hierarchies for symmetric tensors [18]. Our formulations are an extension of these in a different language without requiring symmetry assumptions; moreover, they are complete.

II. THE HIERARCHIES

Let us start by describing our first hierarchy \mathfrak{H}_1 in the basic setting of three particles of the same dimension; the same approach generalizes in a straightforward manner to any number of particles and dimensions. For that,

note that Λ^2 can be written on a two-copy space as

$$\begin{aligned}\Lambda^2(\psi) &= \max_{|abc\rangle} |\langle abc|^{(2)}|\psi\rangle^{(2)}| \\ &= \max_{|abc\rangle} |\langle abc|^{(2)}\Pi_2 \otimes \Pi_2 \otimes \Pi_2|\psi\rangle^{(2)}|.\end{aligned}\quad (2)$$

Clearly, the symmetry of Alice's state allows her to project her state on the symmetric subspace of two particles without changing the value of the above scalar product, i.e., she may apply the projection onto the symmetric space $\Pi_2 = (\mathbb{1} + V)/2$ with the SWAP operator V acting as $V|\psi\rangle|\phi\rangle = |\phi\rangle|\psi\rangle$. The main point is now that while Π_2 acts trivially on the two copies of $|a\rangle$, it acts nontrivially on the two copies of $|\psi\rangle$. The maximum over product states can therefore be relaxed to the norm of the resulting vector,

$$\Lambda^2 \leq \|F_2\| \text{ with } |F_2\rangle = \Pi_2^{\otimes 3}[|\psi\rangle^{\otimes 2}], \quad (3)$$

where we have used $\Pi_2^{\otimes 3}$ to denote $\Pi_2 \otimes \Pi_2 \otimes \Pi_2$ for simplicity. Note that in general the dimensions of the three subsystems do not need to be identical. This approach generalizes naturally to more copies, where the application of the symmetric projector Π_k on k copies of $|\psi\rangle$ leads to the upper bound $\Lambda^2 \leq \|F_k\|^{2/k}$.

The relevant question is whether these upper bounds converge to the correct value of the injective tensor norm Λ^2 . In fact, we show in Appendix A that the hierarchy is complete from both sides; it delivers converging upper and lower bounds. We can directly formulate our first main result:

Observation 1. *For any k , we have the two-sided bound*

$$d_k \|F_k\rangle\|^{2/k} \leq \Lambda^2(\psi) \leq \|F_k\rangle\|^{2/k}, \quad (4)$$

where the coefficients $d_k < 1$ are explicitly known and converge to one, $\lim_{k \rightarrow \infty} d_k = 1$.

In the proof of this observation (given in Appendix A) one expresses the symmetric projectors Π_k by integrals over symmetric pure product states, which allows us to estimate the norm $\|F_k\rangle\|$ by powers of Λ up to some constants incorporated in d_k . This points at a physical interpretation coming from the quantum de Finetti theorem [19–21], which roughly speaking states that a symmetric k -particle quantum state ρ cannot be far away from a product state, that is $\rho \approx \sigma^{\otimes k}$.

The attentive reader will have realized that the estimate used in the transition from Eq. (2) to Eq. (3) is not optimal: The maximization over six-fold product states on the left-hand side of the scalar product was replaced by a maximization over general states, neglecting any product structure. A more careful estimate may keep at least the product structure for a split of the six particles into two groups. Indeed, for such bipartitions, the maximal overlap with $|F_2\rangle$ can directly be computed by considering the Schmidt decomposition of $|F_2\rangle$ [5, 22]. This gives, with small extra effort, an improved bound on Λ^2 for a fixed level of a hierarchy, see also Appendix B.

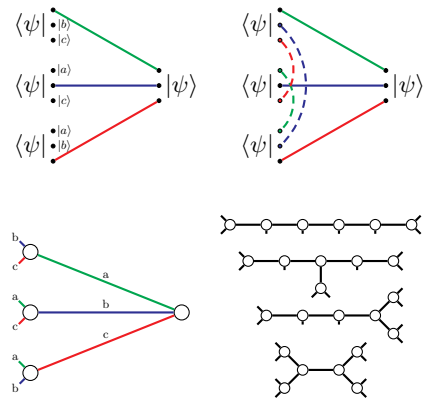


FIG. 1. Graphical description of the possible estimates in the second hierarchy \mathfrak{H}_2 . Upper left: a visualization of Eq. (5). Upper right: relaxation from product states; the dashed lines denote the application of a projector onto the symmetric subspace. Lower left: resulting connectivity graph; the short legs denote the indices on which the symmetric projector acts. Lower right: possible connectivity graphs for six copies of a tripartite state. Note that different labelings are possible which may lead to different results.

For formulating the second hierarchy \mathfrak{H}_2 one uses a specific property of the maximization in the definition of Λ^2 . Namely, if two vectors (say, $|b\rangle$ and $|c\rangle$) are fixed, then $\langle bc|\psi\rangle = |\alpha\rangle$ is an unnormalized pure state and the optimal $|a\rangle$ needs to be proportional to $|\alpha\rangle$. This implies that taking the optimal $|b_o c_o\rangle$ enforces $|\alpha\rangle = \Lambda|a_o\rangle$ (up to some phase), leading to $\langle\psi|b_o c_o\rangle\langle\psi|a_o c_o\rangle\langle\psi|a_o b_o\rangle = \Lambda^3(\psi)\langle a_o b_o c_o\rangle$ and therefore

$$\Lambda^4(\psi) = \max_{|abc\rangle} |\langle\psi|bc\rangle\langle\psi|ac\rangle\langle\psi|ab\rangle|\psi\rangle|. \quad (5)$$

Similar to Eq. (2) one can insert now projectors onto symmetric spaces on the two copies of $|a\rangle$ and similarly for the two copies of $|b\rangle$ and $|c\rangle$. Then, one relaxes the optimization by taking the norm of the resulting six-particle vector $|G_4\rangle$. This kind of estimate can be generalized to more copies of $|\psi\rangle$ in different ways, since there are several ways to wire the indices of the tensors corresponding to the states ψ , see Fig. 1 for examples. All possible tree graphs (that is, connected graphs without cycles) lead to a valid multi-copy tensor which gives an upper bound on Λ . We found that in practice path graphs of length k worked well, and will thus use those for the k 'th level in the hierarchy, see Appendix C for more information. The bounds from this approach are tighter than the ones from the first hierarchy since, for a given number of copies of $|\psi\rangle$, the optimization over fewer external indices needs to be relaxed. Analogous completeness results as Observation 1 hold here as well; we refer to Appendix D for a detailed discussion. Furthermore, in Appendix E we explain the relation of our hierarchies \mathfrak{H}_1 and \mathfrak{H}_2 to results known in mathematics.

In the third hierarchy \mathfrak{H}_3 , instead of taking multiple copies of $|\psi\rangle$, we take just one copy of $|\psi\rangle$ and tensor

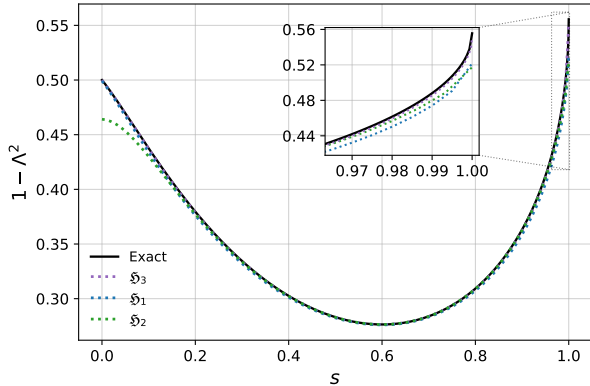


FIG. 2. Lower bounds from the three hierarchies for states of the form $|\psi(s)\rangle = \sqrt{s}|W\rangle + \sqrt{1-s}|GHZ\rangle$. We also show the exact value obtained by solving the one-parameter optimization over symmetric product states [5]. For the first hierarchy \mathfrak{H}_1 we use level 25 and consider the Schmidt decomposition of $|F_k\rangle$ with respect to the bipartition between the first copy and the rest of the copies for improvement. For \mathfrak{H}_2 , for which we only consider the norm and level 10, the used connectivity graph is described in Appendix C. For \mathfrak{H}_3 a level of 60 was used.

product it with $k-1$ identity operators, i.e.,

$$\Lambda^2(\psi) = \max_{|abc\rangle} [\langle abc| \otimes \mathbb{1}^{\otimes k-1}] [\psi \langle \psi| \otimes \mathbb{1}^{\otimes k-1}] [\langle abc| \otimes \mathbb{1}^{\otimes k-1}]. \quad (6)$$

Again, by taking advantage of the fact that the projector on the symmetric subspace can be inserted without changing the above expression, we get an upper bound on Λ^2 by the maximal eigenvalue of the above operator, i.e.,

$$\Lambda^2(\psi) \leq \lambda_{\max}(\Pi_k^{\otimes 3} [\psi \langle \psi| \otimes \mathbb{1}^{\otimes k-1}] \Pi_k^{\otimes 3}). \quad (7)$$

Using the quantum de Finetti theorem, we can prove that the hierarchy \mathfrak{H}_3 is also complete. For the proof and implementation details we refer to Appendices F and G.

III. RESULTS

As a first example of the three hierarchies, we bound the geometric measure for superpositions of the three-qubit W and GHZ state, $|\psi(s)\rangle = \sqrt{s}|W\rangle + \sqrt{1-s}|GHZ\rangle$, with $|W\rangle = (|001\rangle + |010\rangle + |100\rangle)/\sqrt{3}$ and $|GHZ\rangle = (|000\rangle + |111\rangle)/\sqrt{2}$, see also Fig. 2. The levels used for the three hierarchies were 25, 10, and 60, respectively. All three hierarchies are numerically tight for a wide range of s , while the gap increases for the more entangled states. In particular \mathfrak{H}_3 is nearly indistinguishable from the correct value over the whole parameter range.

The hierarchies can also handle larger number of particles. To this end, we show the rates of convergence for the different hierarchies for $|C_5\rangle$, the 5-cycle graph state, in Fig. 3. This state is the maximally entangled state with respect to the geometric measure on five qubits having a value of $E_G = 0.86855$ [23].

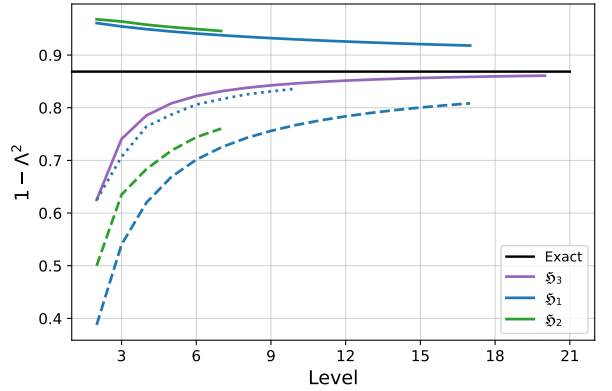


FIG. 3. Bounds on the geometric measure of the 5-cycle graph state $|C_5\rangle$, which is the maximally entangled state w.r.t. the geometric measure for five qubits. The horizontal line at height 0.86855 is the value of the geometric measure of $|C_5\rangle$ [23]. For \mathfrak{H}_1 and \mathfrak{H}_2 we show the upper and lower bounds in solid and dashed, respectively. For \mathfrak{H}_1 we also show the lower bound found by considering the largest Schmidt coefficient of $|F_k\rangle$ with respect to a balanced bipartition between the copies, i.e., the bipartition between the first and second half of the copies. Note that the numerical package ENT-CALC [24] provides for this state only a certified bound in the interval [0.7292, 0.9375].

IV. RELATION TO THE PRODUCT TEST

The construction of the hierarchies above is in close connection to the so-called product test for entanglement [9, 14–16]. For this, one first considers the so-called SWAP test for two particles ρ_{A_1} and ρ_{A_2} , which asks whether the two states are the same and is passed with success probability $1/2 + \text{Tr}(\rho_{A_1} \rho_{A_2})/2 = \text{Tr}(\Pi_2 \rho_{A_1} \otimes \rho_{A_2})$. Then, if two copies of a pure multiparticle state $|\psi\rangle$ are given, one can apply this SWAP test to each pair of particles $A_1 A_2$, $B_1 B_2$ etc. locally and it is clear that the two states pass this test with unit probability if and only if $|\psi\rangle = |a\rangle|b\rangle|c\rangle$ is a product state. Several works investigated the statistical significance of the test for special cases: For two copies of multiparticle states it was shown that the quantity Λ^2 is a lower bound on the passing probability [9], and for two particles and more copies it was demonstrated that the passing probability converges to Λ^2 if the number of copies increases [25].

The completeness of the hierarchy \mathfrak{H}_1 naturally explains and generalizes these results. In fact, $\|F_k\|^2$ can be understood as the probability that the multipartite state $|\psi\rangle$ passes the multi-copy product test and the completeness in Eq. (4) gives upper and lower bounds on this probability in terms of the entanglement of the state (see also Eq. (A9) in Appendix A).

Interestingly, the fact that the hierarchy \mathfrak{H}_2 gives strictly better upper bounds on Λ^2 than \mathfrak{H}_1 (when considering solely the norm in both cases) shows that, if several copies are available, strictly better tests than the

standard multi-copy product test are available.

We note that there are several proposals to implement the product test using quantum circuits [26–28] or randomized measurements [29, 30], these methods are also appropriate for implementing the generalized product tests based on our hierarchies. Finally, we note that the two-copy scenario described above is reminiscent of Bell sampling, where two copies of a state ρ are pairwise measured in the Bell basis [31].

V. APPLICATION TO OPERATORS

Interestingly, the above hierarchies can be adopted also to operators, considering the related notion of the maximal separable numerical range $M(X) = \max_{|a,b,c\rangle} \langle abc|X|abc\rangle$ where X is a general operator [32]. This quantity arises e.g. in the construction of entanglement witnesses and the distillation problem. Generalizing the first hierarchy \mathfrak{H}_1 , one then finds $M^k(X) \leq \lambda_{\max}(\Pi_k^{\otimes 3} X^{\otimes k} \Pi_k^{\otimes 3})$, and a similar statement holds for the third hierarchy \mathfrak{H}_3 .

As a simple, yet nontrivial example for two parties we consider the projector P_{UPB} on an unextendible product basis (UPB) given in [33] (and recounted in Appendix H). Since there is no product vector in the space orthogonal to an UPB, the state $X_{\text{UPB}} \propto \mathbb{1} - P_{\text{UPB}}$ is an entangled state. For the witness construction one needs then the quantity $\delta = M(X_{\text{UPB}})$. Numerically this value was shown to be $\delta \approx 0.97158$ [34], analytically only the bound $\delta \leq 0.998703$ is known [35]. Using the first hierarchy we find for $k = 7$ a bound of $\delta \leq 0.976057$ and with the third hierarchy for $k = 11$ a bound of $\delta \leq 0.973382$, improving in both cases the previous analytical bound significantly.

More generally, the extension to operators sheds some light on the complexity of the separability problem itself. Generally, deciding whether a mixed state admits a separable decomposition is Nondeterministic Polynomial-time (NP) hard [36, 37]. In practice, it can be tackled by semidefinite programming (SDP) hierarchies approximating the separable set [10], where the dimension of the SDP increases in each step of the hierarchy. Consequently, it is clear that $M(X)$ can be computed by considering a similar hierarchy. Our results show, however, that the computation of $M(X)$ (or, equivalently, checking whether a given observable is an entanglement witness) can also be determined by a hierarchy of eigenvalue problems, which may reduce the complexity.

A further possible application considers the optimization over operators. For example, one might consider an SLOCC-class $S_{|\phi\rangle}$ (stochastic local operations and classical communications), consisting of all states that can be reached from $|\phi\rangle$ by SLOCC-operations, i.e., $A_1 \otimes \cdots \otimes A_n |\phi\rangle$. For a given state $|\psi\rangle$ one might be interested in the maximal achievable overlap with states from $S_{|\phi\rangle}$, leading to the value $\max_{A_1 \otimes \cdots \otimes A_n} |\langle \psi | A_1 \otimes \cdots \otimes A_n |\phi\rangle|$. Interestingly, this problem can be rephrased as an optimization over product states, see, e.g., Refs. [38, 39].

VI. GENERALIZATION TO MIXED STATES

So far, we considered the geometric measure for pure states only. In the real world, however, noise is unavoidable, leading to the occurrence of mixed states or density matrices. For such a density matrix ρ the geometric measure is defined via the convex roof construction,

$$E_G(\rho) = \min_{p_k, \psi_k} \sum_k p_k E_G(\psi_k) \quad (8)$$

where the minimum is taken over all decompositions $\rho = \sum_k p_k |\psi_k\rangle\langle\psi_k|$ of the mixed states into pure states ψ_k with some probabilities p_k . Naturally, this minimization is difficult to compute. Upper bounds on $E_G(\rho)$ may be obtained by brute-force numerical optimization, but specifically lower bounds are difficult and only few exact results are known [24, 40, 41].

Taking the viewpoint of a physicist, it is a critical question whether the presented hierarchy can give insights into the quantification of entanglement for mixed states. In the following, using the approach of Ref. [42] we will demonstrate that this is indeed the case. To see this, consider the first step of the hierarchy for three particles, as presented in Eq. (3). This implies that the geometric measure for pure states is bounded by

$$E(\psi) \geq \text{tr}(G_2 \rho^{\otimes 2}) \quad (9)$$

with $G_2 = \mathbb{1} - \Pi_A \otimes \Pi_B \otimes \Pi_C$. If ρ is a mixed state, then any decomposition $\rho = \sum_k p_k |\psi_k\rangle\langle\psi_k|$ is in one-to-one correspondence to a two-copy state $\sigma_{1,2} = \sum_k p_k |\psi_k\rangle\langle\psi_k| \otimes |\psi_k\rangle\langle\psi_k|$ which is separable (with respect to the partition coming from the two copies), in the symmetric subspace and reduces to ρ via $\text{tr}_2(\sigma_{1,2}) = \rho$. So it follows that

$$E(\rho) \geq \min_{\sigma_{1,2}} \text{tr}(G_2 \sigma_{1,2}) \quad (10)$$

s.t.: $\sigma_{1,2}$ separable, symmetric and $\text{tr}_2(\sigma_{1,2}) = \rho$.

The point is that the separability condition can be relaxed by requiring that $\sigma_{1,2}$ is only PPT with respect to the $1|2$ partition and the resulting lower bound can be directly computed via semidefinite programming (SDP). This approach can be generalized to higher orders of our hierarchy or to other relaxations of the separability constraint in Eq. (10). Note finally that there are other approaches that can be used to convert our results for pure states to characterizing mixed states [43].

In fact, already the simple PPT relaxation of the lowest order in Eq. (10) gives surprisingly strong criteria for entanglement. As a first example, we considered GHZ states mixed with white noise $\rho(p) = p|\text{GHZ}\rangle\langle\text{GHZ}| + (1-p)\mathbb{1}/8$. These are known to be entangled if and only if $p > 1/5$ [44, 45] and the SDP directly reproduced this threshold. The second example are W states mixed with noise, $\rho(p) = p|W\rangle\langle W| + (1-p)\mathbb{1}/8$. These states are known to be fully separable for $p \leq 0.177$, entangled for

$p > \sqrt{3}/(8 + \sqrt{3}) \approx 0.1778$, but still separable for any bipartition until $p \leq 0.2095$ [46]. This means that entanglement in the regime $p \in [0.1778, 0.2095]$ cannot be detected by any bipartite criterion, such as the PPT criterion. Our SDP, however, directly allows to detect the entanglement already with the second level of the hierarchy for all $p \geq 0.1781$, demonstrating the ability to detect also weakly entangled states in a straightforward manner. Finally, the three-qubit Tao state τ —which is the most robust entangled state that is biseparable for any bipartition [47]—can be detected in a parameter regime where all other known criteria fail, further details can be found in Appendix I. Finally, we add that the presented approach can also be used to characterize the convex roof of other entanglement monotones [48, 49] which attracted some attention recently and have a formal similarity to the steps of the hierarchies.

VII. DISCUSSION

We introduced three different hierarchies for the geometric measure of entanglement and showed their convergence, considering multiple copies of the target state and applying different symmetrization arguments. On the mathematical side, this implies a characterization of the injective tensor norm as a limit of the 2-norms of a family of vectors. On the physical side, this leads to easily computable upper and lower bounds on the geometric measure of entanglement. We find that the first hierarchy \mathfrak{H}_1 connects closely with the product test, extending results known for the bipartite case to the multipartite setting. The third hierarchy we find to provide the best lower bounds in practice.

An interesting open question, which initiated also the mathematical discussion [17], is whether the hierarchies can also be interpreted in a combinatorial way. The known upper bound for symmetric matrices can be understood as counting the closed walks in a weighted graph, where the weights are described by the matrix. For the case of complex tensors, such an interpretation requires still some work, but may result in an abundant

source of further inspiration.

A more physical application is the maximization of state overlaps over local unitaries, which is also an optimization over product structures. The hierarchies seem to be relevant also in this case, although a more detailed analysis is needed. For example, in the case of unitary qubit operators one optimizes implicitly over real instead of complex states [50], so it might be worth investigating further the relationship between the optimization over real and complex states. Mathematically, the geometric measure can also be seen as the minimal distance of a higher rank tensor to the rank-1 tensors. Naturally, this can be generalized to higher ranks, for example, asking for the best rank-2 approximation of a given tensor. It would be interesting to investigate whether similar hierarchies can be formulated for these cases.

Acknowledgments—We thank Sophia Denker, Shmuel Friedland, Sev Gharibian, Ties-Albrecht Ohst, Jordi Romero-Pallejà, Dorian Rudolph, and Rene Schwonnek for discussions. This work was supported by the Deutsche Forschungsgemeinschaft (DFG, German Research Foundation, project number 563437167), the Sino-German Center for Research Promotion (Project M-0294), and the German Federal Ministry of Research, Technology and Space (Project QuKuK, Grant No. 16KIS1618K and Project BeRyQC, Grant No. 13N17292). LTW acknowledges the support from the House of Young Talents of the University of Siegen. AR acknowledges financial support from Spanish MICIN (projects: PID2022; 141283NBI00; 139099NBI00) with the support of FEDER funds, the Spanish Government with funding from European Union NextGenerationEU (PRTR-C17.I1), the Generalitat de Catalunya, the Ministry for Digital Transformation and of Civil Service of the Spanish Government through the QUANTUM ENIA project -Quantum Spain Project- through the Recovery, Transformation and Resilience Plan Next-Generation EU within the framework of the Digital Spain 2026 Agenda. KG acknowledges the support from the Alexander von Humboldt Foundation. XDY acknowledges the support from the National Natural Science Foundation of China (Grants No. 12574537 and No. 12205170) and the Shandong Provincial Natural Science Foundation of China (Grant No. ZR2022QA084).

APPENDIX

We prove in Appendix A the completeness of the first hierarchy \mathfrak{H}_1 ; in Appendix B we show how to reduce the computation time and include the restriction to PPT states for \mathfrak{H}_1 . Appendix C contains the implementation details for the second hierarchy \mathfrak{H}_2 , and we prove its completeness in Appendix D. We detail the connection between our results and the ideas from H. A. Helfgott and S. Friedland in Appendix E. Completeness and implementation details of the third hierarchy \mathfrak{H}_3 are shown in Appendices F and G. Appendix H discusses how hierarchies \mathfrak{H}_1 and \mathfrak{H}_3 can be used to find the separable numerical range of operators. We conclude by finding lower bounds on the convex roof extension of E_G for mixed states in Appendix I.

Appendix A: The first hierarchy \mathfrak{H}_1 : proof of Observation 1

Observation 1. Given an n -partite state $|\psi\rangle$, and for any k , we have the two-sided bound

$$d_k \| |F_k\rangle\|^{2/k} \leq \Lambda^2(\psi) \leq \| |F_k\rangle\|^{2/k}, \quad (\text{A1})$$

where the coefficients $d_k := \binom{k+d-1}{k}^{-n/k} < 1$ converge to one, $\lim_{k \rightarrow \infty} d_k = 1$.

Proof. For a general number of copies k , we define $|F_k\rangle = \Pi_k \otimes \Pi_k \otimes \Pi_k [|\psi\rangle^{\otimes k}]$, where the k -copy symmetric projector is given by $\Pi_k = \sum_{\pi \in S_k} V_\pi / k!$ with S_k being the symmetric group of k -element permutations π and V_π their representation on $(\mathbb{C}^d)^{\otimes k}$. This definition for three-partite states extends naturally to n -partite states, through $|F_k\rangle = \Pi_k^{\otimes n} [|\psi\rangle^{\otimes k}]$.

As sketched in the main text, we first note that

$$\begin{aligned} \Lambda(\psi) &:= \max_{\phi \in \text{SEP}} |\langle \phi | \psi \rangle| \\ &= \max_{\phi \in \text{SEP}} |\langle \phi |^{\otimes k} | \psi \rangle^{\otimes k}|^{1/k} \\ &= \max_{\phi \in \text{SEP}} |\langle \phi |^{\otimes k} \Pi_k^{\otimes n} | \psi \rangle^{\otimes k}|^{1/k} \\ &\leq \max_{\Phi \in (\mathbb{C}^d)^{nk}} |\langle \Phi | \Pi_k^{\otimes n} | \psi \rangle^{\otimes k}|^{1/k} \\ &= \| |F_k\rangle\|^{1/k}. \end{aligned} \quad (\text{A2})$$

The third equality holds because $\Pi_k^{\otimes n} |\phi\rangle^{\otimes k} = |\phi\rangle^{\otimes k}$ for any separable state $|\phi\rangle$. The inequality holds because the maximization over general states $|\Phi\rangle$ contains in particular $|\phi\rangle \in \text{SEP}$, and the next equality holds because the state $|\Phi\rangle$ with maximal overlap with $|F_k\rangle$ is proportional to it, $|\Phi\rangle \propto |F_k\rangle$. This proves the right-hand-side inequality in Observation 1.

To prove the left-hand-side inequality in Observation 1, we will write the symmetric projector as

$$\Pi_k = \binom{k+d-1}{k} \int_{\phi \in \text{Haar}} |\phi\rangle \langle \phi|^{\otimes k} d\phi, \quad (\text{A3})$$

where Haar is the flat Haar-random measure on pure states in \mathbb{C}^d [51]. Therefore, n copies of Π_k read

$$\Pi_k^{\otimes n} = \binom{k+d-1}{k}^n \int_{\phi_1, \dots, \phi_n \in \text{Haar}} |\phi_1 \dots \phi_n\rangle \langle \phi_1 \dots \phi_n|^{\otimes k} d\phi_1 \dots d\phi_n. \quad (\text{A4})$$

Denote $|a_1 \dots a_n\rangle$ the closest separable state to $|\psi\rangle$, namely $\Lambda(\psi) = |\langle a_1 \dots a_n | \psi \rangle|$. Then the norm $\| \Pi_k^{\otimes n} |\psi\rangle^{\otimes k} \|^2$ reads

$$\begin{aligned} \| \Pi_k^{\otimes n} |\psi\rangle^{\otimes k} \|^2 &= \langle \psi |^{\otimes k} \Pi_k^{\otimes n} | \psi \rangle^{\otimes k} \\ &= \binom{k+d-1}{k}^n \int_{\phi_1, \dots, \phi_n \in \text{Haar}} |\langle \phi_1 \dots \phi_n | \psi \rangle|^2 d\phi_1 \dots d\phi_n \\ &\leq \binom{k+d-1}{k}^n |\langle a_1 \dots a_n | \psi \rangle|^{2k} \int_{\phi_1, \dots, \phi_n \in \text{Haar}} d\phi_1 \dots d\phi_n \\ &= \binom{k+d-1}{k}^n |\langle a_1 \dots a_n | \psi \rangle|^{2k} \\ &= \binom{k+d-1}{k}^n \Lambda^{2k}(\psi) \end{aligned} \quad (\text{A5})$$

since $\int_{\phi_1, \dots, \phi_n \in \text{Haar}} d\phi_1 \dots d\phi_n = 1$. Taking the k 'th root at both sides we have that

$$\| \Pi_k^{\otimes n} |\psi\rangle^{\otimes k} \|^2/k \leq \binom{k+d-1}{k}^{n/k} \Lambda^2(\psi). \quad (\text{A6})$$

Defining $d_k := \binom{k+d-1}{k}^{-n/k}$, and observing that $d_k < 1$ for finite k by definition, this means that

$$d_k \||F_k\rangle\|^{2/k} \leq \Lambda^2(\psi), \quad (\text{A7})$$

which proves the left-hand-side inequality in Observation 1.

It is only left to see convergence of the hierarchy, namely that d_k tends to 1 in the limit $k \rightarrow \infty$. For this we note that the expression $\binom{k+d-1}{k} = \frac{1}{(d-1)!} \prod_{i=1}^{d-1} (k+i)$ is a polynomial in k of degree $d-1$, so the leading terms of d_k are of the order $k^{-\frac{d}{k}}$. We therefore find

$$d_k = \binom{k+d-1}{k}^{-n/k} = O\left(k^{-\frac{d}{k}}\right) \rightarrow 1 \text{ for } k \rightarrow \infty. \quad (\text{A8})$$

Therefore the hierarchy is convergent for finite dimension d and number of parties n . \square

Note that the above observation can also be phrased as bounding the norm $\||F_k\rangle\|$, which is related to the acceptance probability in the context of the product test. In this formulation the result reads

$$\Lambda^{2k}(\psi) \leq \||F_k\rangle\|^2 \leq \frac{1}{(d_k)^{2k}} \Lambda^{2k}(\psi). \quad (\text{A9})$$

Appendix B: The first hierarchy \mathfrak{H}_1 : Numerical approach

We demonstrate here how the bounds from first hierarchy can be calculated in practice, using the three-qubit case as an example.

1. Calculating the norms of $|F_k\rangle$

In the first hierarchy, we consider the vector $|F_k\rangle = \Pi_k \otimes \Pi_k \otimes \Pi_k [|\psi\rangle^{\otimes k}]$. As this vector is symmetric on every subsystem A, B, and C, it can be written as $|F_k\rangle = \sum_{ijl} c_{ijl} |D_k^i\rangle |D_k^j\rangle |D_k^l\rangle$, where $|D_k^i\rangle = \frac{1}{N_i} \sum_{\pi \text{ perm.}} \pi(|0\rangle^{\otimes i} \otimes |1\rangle^{\otimes (k-i)})$ are the Dicke states. The sum runs over all distinct permutations of $|0\rangle^{\otimes i} \otimes |1\rangle^{\otimes (k-i)}$ and the normalization constant is then given by $N_i^2 = \binom{k}{i}$. As these states form a basis, we need effectively only to compute the overlaps $c_{ijk} = |\langle \psi |^{\otimes k} |D_k^i\rangle |D_k^j\rangle |D_k^l\rangle|$.

We start by considering a single qubit state $|\phi\rangle$ and the coefficient $\langle \phi^{\otimes k} | D_k^i \rangle$. Noticing that the Schmidt decomposition of a Dicke state for the bipartite cut between one party and the rest is given by $|D_k^i\rangle = \sqrt{\frac{i}{k}} |0\rangle \otimes |D_{k-1}^{i-1}\rangle + \sqrt{\frac{k-i}{k}} |1\rangle \otimes |D_{k-1}^i\rangle$ we directly find the iterative rule

$$\langle \phi^{\otimes k} | D_k^i \rangle = \sqrt{\frac{i}{k}} \langle \psi | 0 \rangle \langle \phi^{\otimes k-1} | D_{k-1}^{i-1} \rangle + \sqrt{\frac{k-i}{k}} \langle \psi | 1 \rangle \langle \phi^{\otimes k-1} | D_{k-1}^i \rangle. \quad (\text{B1})$$

Using this rule one may calculate the coefficients of $|\phi\rangle^{\otimes k}$ with respect to the Dicke basis iteratively while only considering vectors of length up to $k+1$, reducing the computational effort drastically. This approach generalizes straightforwardly to the multipartite case of n parties, where one then has to consider only vectors of length up to $(k+1)^n$. Finally, the norm $\||F_k\rangle\|$ can then be directly calculated by $\sum_{i,j,l} |c_{ijl}|^2$.

2. Including PPT in the hierarchies

As noted in the main text, the three different hierarchies give upper bounds on the geometric measure by relaxing the optimization over product states to arbitrary states. One may, however, retain some of the structure of the product states in the optimization by considering states which have a positive partial transpose (PPT) with respect to a (or every) bipartition, which leads to improved bounds. As an example, we demonstrate here how this approach can be implemented in the first hierarchy \mathfrak{H}_1 .

In the first hierarchy, we have for $k = 2$

$$\Lambda^4(\psi) = \max_{|abc\rangle} |\langle abc|^{\otimes 2} |F_2\rangle|^2 = \max_{\sigma \in \text{SEP}} \text{Tr}[|F_2\rangle\langle F_2|\sigma] \leq \max_{\sigma \in \text{SEP}(S|\bar{S})} \text{Tr}[|F_2\rangle\langle F_2|\sigma] \leq \||F_2\rangle\|^2 \quad (\text{B2})$$

with $|F_2\rangle = \Pi_2 \otimes \Pi_2 \otimes \Pi_2 [|\psi\rangle^{\otimes 2}]$, where SEP and $\text{SEP}(S|\bar{S})$ denote all fully separable states and all states which are separable with respect to a fixed bipartition $S|\bar{S}$ of the two-copy space $A_1B_1C_1A_2B_2C_2$. For a bipartite state the maximal achievable overlap with a separable state is given by the largest Schmidt coefficient. Note, however, that the vector $|F_2\rangle$ is not normalized, so instead we find as an upper bound $\text{Tr}[|F_2\rangle\langle F_2|\sigma] \leq s_{\max}^{S|\bar{S}}$ for σ separable across the bipartition, where $s_{\max}^{S|\bar{S}}$ denotes the largest singular value of the reduced density matrix $\text{Tr}_{\bar{S}}[|F_2\rangle\langle F_2|]$.

These arguments generalize to the case of multiple parties and copies, leading to various possible bipartitions one could consider for an upper bound on $\Lambda(\psi)$. In the examples considered in this paper, we implemented two different fixed bipartitions. The first is given by considering the cut between the first copy and all other copies, while the second describes the cut between the first half and the second half of the k copies. As the calculation of the largest singular value depends on the size of the reduced density matrix across the cut, the second bipartition is numerically more demanding than the first. However, the second bipartition leads typically to better upper bounds than every other bipartition for randomly chosen states.

We show here shortly how the Schmidt coefficients can be calculated in practice for three-qubit states for the bipartition between the first copy and the remaining copies. Note that the Friedland state $|F_k\rangle$ can be written as $|F_k\rangle = \sum_{ijl} c_{ijl} |D_k^i D_k^j D_k^l\rangle$. The Schmidt coefficient is then given by the maximal eigenvalue of $\text{Tr}_{A_2 \dots A_k B_2 \dots B_k C_2 \dots C_k} [|F_k\rangle\langle F_k|]$. For the Dicke states the reduced density matrix can be calculated directly as

$$\Delta(k; \alpha, \beta) := \text{Tr}_{2, \dots, k} (|D_k^\alpha\rangle\langle D_k^\beta|) = \frac{1}{n} \begin{pmatrix} \alpha \delta_{\alpha, \beta} & \sqrt{\alpha(k-\beta)} \delta_{\alpha, \beta+1} \\ \sqrt{\beta(k-\alpha)} \delta_{\alpha, \beta-1} & (k-\alpha) \delta_{\alpha, \beta} \end{pmatrix}, \quad (\text{B3})$$

leading to

$$\text{Tr}_{A_2 \dots A_k B_2 \dots B_k C_2 \dots C_k} [|F_k\rangle\langle F_k|] = \sum_{ijl, \alpha \beta \gamma} c_{ijl}^* c_{\alpha \beta \gamma} \Delta(k; i, \alpha) \otimes \Delta(k; j, \beta) \otimes \Delta(k; l, \gamma). \quad (\text{B4})$$

This also is generalizable to more parties, thus, the calculation of the Schmidt coefficients from given coefficients $c_{ij\dots}$ only amounts to the eigenvalue decomposition of a $2^n \times 2^n$ matrix. The computational important step is the construction of this matrix from the coefficients $c_{ij\dots}$, as the number of these grows as k^n . In practice, this scheme was for $k \leq 25$ in comparison not much slower than calculating the norm, while leading to a better upper bound.

Appendix C: The second hierarchy \mathfrak{H}_2 : Numerical approach

The trees that arise in the second hierarchy can be interpreted as tree tensor networks (TTNs) [52], whose individual tensors are copies of the state $|\psi\rangle$ under consideration. Two examples for four particles and four copies are given in Fig. 4.

The first example shown is a finite Bethe lattice. The infinite Bethe lattice is the infinite n -regular tree, while the finite variant of level l arises from the infinite one by choosing a root vertex and taking the induced subgraph on the vertices that are a distance at most l from that root. The Bethe lattice is natural, since it does not favor any of the particles over the other. However, in practice we found that the bounds found through Bethe lattice TTNs were rather weak. Furthermore, the number of tensors grows exponentially in the parameter l , making runtime prohibitive for $l > 2$.

In practice we found that the second example of path graph TTNs worked well in practice. However, unlike the Bethe lattice, for each level k there are different ways to connect the labeled legs for a given path graph. A path graph TTN can then be specified by the sequence of legs that get connected. For example, the path graph TTN in Fig. 4 is specified by $[1, 3, 2]$, when starting from the top tensor. The different choices for fixed k yielded similar results, but sequences of the form $[1, 2, \dots, n, 1, 2, \dots, n, 1, \dots]$ worked well in practice.

For completeness, we show the bounds for different path graph TTNs. In particular, we consider superpositions of Dicke states with single and double excitations, i.e. $\sqrt{s}|D_1^{(5)}\rangle + \sqrt{1-s}|D_2^{(5)}\rangle$. We observe here once more that the bounds are less tight for the more strongly entangled states.

Appendix D: The second hierarchy \mathfrak{H}_2 : proof of convergence

A similar approach as to the first hierarchy can be used for the second hierarchy. In the following, we denote by $|T\rangle$ the tree tensor network (see Appendix C), by $k(i)$ the number of open legs of a given type i in the tree T , by

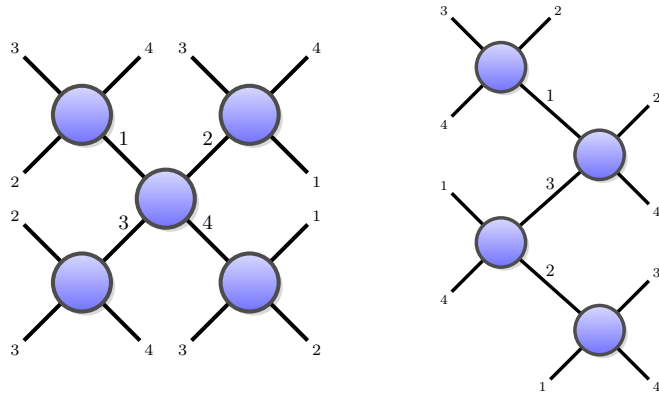


FIG. 4. Examples of graphs corresponding to the second hierarchy for $n = 4$ particles. (Left). First non-trivial level $l = 1$ of the finite Bethe lattice, where an initial tensor is contracted with n copies. Subsequent levels of the Bethe lattice contract each of the tensors in the ‘outer’ layer with $n - 1$ other copies. (Right) Example tree tensor network of a path graph labeled by $[1, 3, 2]$, corresponding to the indices connecting the tensors from top to bottom. To calculate the associated bound for a given tree tensor network, we apply symmetric projectors on each of the open legs of a given type, and then contract the tensor with itself. Note that the symmetric projectors can be of different sizes; the tree tensor network on the right requires a symmetric projector on 2 copies for the leg of type 1, while requiring a symmetric projector on 4 copies for the leg of type 4.

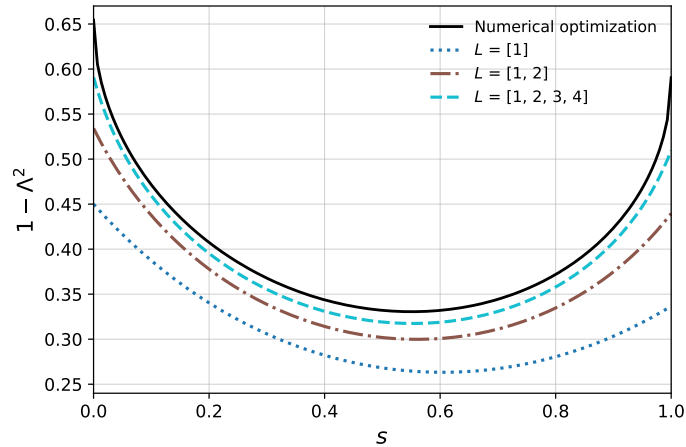


FIG. 5. Lower bounds on the geometric measure of superpositions of Dicke states of the form $\sqrt{s}|D_1^{(5)}\rangle + \sqrt{1-s}|D_2^{(5)}\rangle$. The lower bounds are found for three path graph TTNs parametrized by $L = [1]$, $L = [1, 2]$, $L = [1, 2, 3, 4]$. We also show a numerical upper bound, found by a brute-force search over a discretization of all symmetric product states.

$\Pi_{k(i)}$ the projector onto the symmetric subspace of the legs of type i , and by k the total number of vertices/‘copies’ in T . We then have the following.

Theorem 2. *Given an n -partite state $|\psi\rangle$ and any associated $|T\rangle$ with k vertices, and $k(i)$ open legs of each type i , we have the two-sided bound*

$$d_k \cdot \left\| \bigotimes_{i=1}^n \Pi_{k(i)} |T\rangle \right\|^{2/k} \leq \Lambda^2(\psi) \leq \left\| \bigotimes_{i=1}^n \Pi_{k(i)} |T\rangle \right\|^{2/k}, \quad (D1)$$

for any k . The coefficient $d_k := \left(\prod_{i=1}^n \binom{k(i)+d-1}{k(i)} \right)^{-1/k} < 1$ converges to one, i.e. $\lim_{k \rightarrow \infty} d_k = 1$.

Proof. Let $|a_1 \dots a_n\rangle$ be the closest separable state to $|\psi\rangle$. Since by definition $|\langle a_1 \dots a_n | \psi \rangle| = \Lambda$, we have that $\langle \psi | a_2 \dots a_n \rangle = \Lambda |a_1\rangle$ up to some phase. Similar statements hold for the other $|a_i\rangle$ as well.

As such, we can rewrite the norm as

$$\Lambda(\psi)^k = \max_{a_1, \dots, a_n \in \text{SEP}} \left| \langle a_1 |^{\otimes k(1)} \dots \langle a_n |^{\otimes k(n)} |T \rangle \right| \quad (\text{D2})$$

$$= \max_{a_1, \dots, a_n \in \text{SEP}} \left| \langle a_1 |^{\otimes k(1)} \dots \langle a_n |^{\otimes k(n)} \bigotimes_{i=1}^n \Pi_{k(i)} |T \rangle \right| \quad (\text{D3})$$

$$\leq \left\| \bigotimes_{i=1}^n \Pi_{k(i)} |T \rangle \right\|. \quad (\text{D4})$$

In the first step, we used that every leaf v of T has a unique leg that is not open. This implies that $\langle a_1 \dots a_{j-1} a_j a_{j+1} \dots a_n | T \rangle = \Lambda | T' \rangle$ (up to a phase). Here j is the type of the non-open leg of v , and T' is the tree tensor network T but with v deleted. By removing leaves recursively, the claim follows. In the last line we use that the maximization can be upper bounded by the norm. This proves the upper bound.

For the lower bound, we use that

$$\begin{aligned} \left\| \bigotimes_{i=1}^n \Pi_{k(i)} |T \rangle \right\|^2 &= \left(\prod_{i=1}^n \binom{k(i) + d - 1}{k(i)} \right) \int_{\phi_1, \dots, \phi_n \in \text{Haar}} \left\| \langle \phi_1^{\otimes k(1)} \dots \phi_n^{\otimes k(n)} | T \rangle \right\|^2 d\phi_1 \dots d\phi_n \\ &\leq \left(\prod_{i=1}^n \binom{k(i) + d - 1}{k(i)} \right) \left\| \langle a_1^{\otimes k(1)} \dots a_n^{\otimes k(n)} | T \rangle \right\|^2 \\ &= \left(\prod_{i=1}^n \binom{k(i) + d - 1}{k(i)} \right) \Lambda^{2k}(\psi). \end{aligned} \quad (\text{D5})$$

As before, it now remains to show that

$$\left(\prod_{i=1}^n \binom{k(i) + d - 1}{k(i)} \right)^{1/k} \leq \left(\frac{k + d - 1}{d - 1} \right)^{n/k} \xrightarrow{k \rightarrow \infty} 1. \quad (\text{D6})$$

where in the first step we used that $\binom{k(i) + d - 1}{k(i)} = \binom{k(i) + d - 1}{d - 1} \leq \binom{k + d - 1}{d - 1}$ since $k(i) \leq k$, and in the second step we used the same argument as in Eq. (A8). \square

Appendix E: Relation to the works by H. A. Helfgott and S. Friedland

This present work is inspired by the work of S. Friedland [18] which is itself a comment on a question by H. A. Helfgott [17]. So, in this Appendix, we want to explain this background and shortly show the connections to these works.

Interpreting a bipartite state $|\psi\rangle$ as a matrix ψ_{ij} we find that $\max_{|ab\rangle} |\langle \psi | ab \rangle|$ exactly amounts to the injective matrix norm $\|\psi\|_{\text{inj}} = \max_{a,b} |\sum_{ij} \psi_{ij} a_i b_j|$. Note that for matrices this also equals the largest singular value or Ky-Fan norm. The definition directly generalizes to the tensor case. Note that the maximization here depends on the chosen underlying field, which can be either real or complex. As an example consider the three-qubit state $|B\rangle = \frac{1}{2}(|001\rangle + |010\rangle + |100\rangle - |111\rangle)$, which has $\|\psi\|_{\text{inj}, \mathbb{R}} = \frac{1}{2} < \frac{1}{\sqrt{2}} = \|\psi\|_{\text{inj}, \mathbb{C}}$ [53].

We now consider the real case first. In the case of real symmetric matrices it follows from the eigenvalue decomposition that

$$\|\psi\|_{\text{inj}}^k \leq \text{Tr}[\psi^k]. \quad (\text{E1})$$

This can be interpreted in a combinatorial way, as $\text{Tr}[\psi^k]$ counts the weight of all closed walks of length k in a weighted directed graph with adjacency matrix ψ , see for example Theorem 2.13 of [54]. Note also that one can rewrite $\text{Tr}[\psi^k]$ for symmetric ψ using multiple copies of ψ in the following way. For instance, for $k = 3$ one has $\text{Tr}[\psi^k] = \sum_{ijrs} \psi_{ir} \psi_{rs} \psi_{sj} = \sum_{kp} (\sum_{lmno} \delta_{ln} \delta_{mo} \psi_{kl} \psi_{mn} \psi_{op})$, which bears some resemblance to the construction of the second hierarchy in the main text.

In Ref. [18] mainly real symmetric tensors were considered. For them, two hierarchies were constructed, in analogy to \mathfrak{H}_1 and \mathfrak{H}_2 in the main text. For \mathfrak{H}_2 , only graphs where the underlying tree is a regular tree (also called Bethe lattice) were used. These graphs can be constructed by taking a "root node", and connect it to n nodes in the first layer. In the second layer one connects each of the n nodes to $n - 1$ new nodes, and repeats this scheme for every

further layer. See also Fig. 4 and the description in Appendix C. Note that in the case of symmetric tensors, the optimizing vectors in the injective norm can be assumed to be symmetric, i.e., $\|\psi\|_{\text{inj}} = \max_a \langle \psi | a a \dots \rangle$ [55, 56].

It was then shown that in the real case the first hierarchy converges $\lim_{k \rightarrow \infty} \|F_k\|^{1/k} =: \rho_{1,\mathbb{R}}(\psi) \geq \|\psi\|_{\text{inj},\mathbb{R}}$ for symmetric tensors, and the second hierarchy likewise converges to a finite value $\rho_2(\psi) \geq \|\psi\|_{\text{inj},\mathbb{R}}$. In both cases equality holds for orthogonally diagonalizable tensors, i.e., tensors of the form

$$|\phi\rangle = \sum_i \lambda_i |a_i a_i \dots\rangle, \quad (\text{E2})$$

where the $|a_i\rangle$ form local orthonormal bases.

Our results now demonstrate that in the complex case (which was also shortly mentioned in [18]) $\rho_{1,\mathbb{C}}(\psi) = \rho_{2,\mathbb{C}}(\psi) = \|\psi\|_{\text{inj},\mathbb{C}}$.

Additionally, our results also seem to indicate that the value $\rho_{1,\mathbb{R}}(\psi)$ is exactly given by the complex injective tensor norm $\|\psi\|_{\text{inj},\mathbb{C}}$ for any real symmetric tensor ψ . This follows from the fact that in the first hierarchy we only compute the norm of the symmetrized tensor ψ_{ijk} , where in the case of a real tensor all coefficients are real, leading therefore to the same value in both the real and complex hierarchy. Since we show that the complex hierarchy converges exactly to the complex injective tensor norm, the same should hold for the real hierarchy. Thus, we find the seemingly strange phenomenon that a hierarchy defined on real symmetric tensors converges to their complex norm, i.e., $\lim_{k \rightarrow \infty} \|F_k\|^{1/k} = \rho_{1,\mathbb{R}}(\psi) = \|\psi\|_{\text{inj},\mathbb{C}} \geq \|\psi\|_{\text{inj},\mathbb{R}}$, where the inequality in the last step might be gapped for a given state, see the example of $|B\rangle$ above.

Appendix F: The third hierarchy \mathfrak{H}_3 : proof of convergence

Let us first use the symmetric case to illustrate the idea. Let $|\psi\rangle$ be a symmetric state in $\mathcal{H}^{\otimes n}$ and $\Lambda(\psi) = \max |\langle \psi | x^{\otimes n} \rangle| = \max_{\rho \in \text{SEP} \cap \text{SYM}} \text{Tr}(|\psi\rangle\langle \rho|)$, where $|x\rangle \in \mathcal{H}$, where $\rho \in \text{SEP} \cap \text{SYM}$ means that ρ is a separable state in the symmetric subspace. Now, we take advantage of the quantum de Finetti theorem, or the so-called symmetric extension, and approximate ρ with the reduced states of symmetric states $\rho_{(k+n)}$ in $\mathcal{H}^{\otimes k+n}$. Specifically, let ξ_k be the solution of the following SDP

$$\begin{aligned} \max_{\rho} \quad & \text{Tr} [(\mathbb{1}^{\otimes k} \otimes |\psi\rangle\langle \psi|) \rho_{k+n}] \\ \text{s.t.} \quad & \Pi_{k+n} \rho_{k+n} \Pi_{k+n} = \rho_{k+n}, \\ & \rho_{k+n} \geq 0, \quad \text{Tr}(\rho_{k+n}) = 1, \end{aligned} \quad (\text{F1})$$

then $\xi_k \geq \xi_{k+1}$ and $\lim_{k \rightarrow \infty} \xi_k = \max |\langle \psi | x^{\otimes n} \rangle|$. One can easily verify that Eq. (F1) can be solved analytically as

$$\begin{aligned} \xi_k &= \lambda_{\max} (\Pi_{k+n} (\mathbb{1}^{\otimes k} \otimes |\psi\rangle\langle \psi|) \Pi_{k+n}) \\ &= \lambda_{\max} (\Pi_{k+n} (\Pi_k \otimes |\psi\rangle\langle \psi|) \Pi_{N+n}). \end{aligned} \quad (\text{F2})$$

Generally, we consider the problem of optimizing $\max_{\rho_{ABC} \in \text{SEP}} \text{Tr}(X_{ABC} \rho_{ABC})$, where X_{ABC} is some fixed Hermitian matrix. In this case, we can still apply the symmetric extension but to each subsystem individually, and the obtained hierarchy is still complete [57], i.e., the solutions ξ_k of the following SDPs give a complete hierarchy:

$$\begin{aligned} \max_{\rho} \quad & \text{Tr} [(\mathbb{1}_A^{\otimes k-1} \otimes \mathbb{1}_B^{\otimes k-1} \otimes \mathbb{1}_C^{\otimes k-1} \otimes X_{ABC}) \rho_k] \\ \text{s.t.} \quad & \Pi_k^A \otimes \Pi_k^B \otimes \Pi_k^C \rho_k \Pi_k^A \otimes \Pi_k^B \otimes \Pi_k^C = \rho_k, \\ & \rho_k \geq 0, \quad \text{Tr}(\rho_k) = 1, \end{aligned} \quad (\text{F3})$$

where $\rho_k \in \mathcal{H}_A^{\otimes k} \otimes \mathcal{H}_B^{\otimes k} \otimes \mathcal{H}_C^{\otimes k}$ and Π_k^A , Π_k^B , and Π_k^C are symmetric projectors on $\mathcal{H}_A^{\otimes k}$, $\mathcal{H}_B^{\otimes k}$, and $\mathcal{H}_C^{\otimes k}$, respectively. Similarly, one can easily verify that Eq. (F3) can be solved analytically as

$$\begin{aligned} \xi_k &= \lambda_{\max} [\Pi_k^A \otimes \Pi_k^B \otimes \Pi_k^C (\mathbb{1}_A^{\otimes k-1} \otimes \mathbb{1}_B^{\otimes k-1} \otimes \mathbb{1}_C^{\otimes k-1} \otimes X_{ABC}) \Pi_k^A \otimes \Pi_k^B \otimes \Pi_k^C] \\ &= \lambda_{\max} [\Pi_k^A \otimes \Pi_k^B \otimes \Pi_k^C (\Pi_A^{\otimes k-1} \otimes \Pi_B^{\otimes k-1} \otimes \Pi_C^{\otimes k-1} \otimes X_{ABC}) \Pi_k^A \otimes \Pi_k^B \otimes \Pi_k^C]. \end{aligned} \quad (\text{F4})$$

Appendix G: The third hierarchy \mathfrak{H}_3 : numerical approach

To show how the third hierarchy can be efficiently calculated, we take the qubit case ($\dim(\mathcal{H}) = 2$) as an example. Still, we first consider the symmetric case. For any n -qubit symmetric pure state $|\psi\rangle$, we have

$$|\psi\rangle = \sum_{j=0}^n a_j |D_n^j\rangle, \quad (G1)$$

$$\Pi_k = \sum_{\alpha=0}^k |D_k^\alpha\rangle\langle D_k^\alpha|, \quad (G2)$$

$$\Pi_k \otimes |\psi\rangle\langle\psi| = \sum_{\alpha=0}^k |D_k^\alpha\psi\rangle\langle D_k^\alpha\psi|, \quad (G3)$$

where $|D_k^i\rangle$ are the Dicke states. Then,

$$\begin{aligned} \Pi_{k+n} |D_k^\alpha\psi\rangle &= \sum_{j=0}^n a_j \Pi_{k+n} |D_k^\alpha D_n^j\rangle \\ &= \sum_{j=0}^n a_j \sqrt{\frac{\binom{k}{\alpha} \binom{n}{j}}{\binom{k+n}{\alpha+j}}} |D_{k+n}^{\alpha+j}\rangle \\ &= \sum_{\ell=0}^{k+n} a_{\ell-\alpha} \mu_{\alpha\ell} |D_{k+n}^\ell\rangle, \end{aligned} \quad (G4)$$

where

$$\mu_{\alpha\ell} := \sqrt{\frac{\binom{k}{\alpha} \binom{n}{\ell-\alpha}}{\binom{k+n}{\ell}}}, \quad (G5)$$

and we have assumed that as $a_{\ell-\alpha} = \mu_{\alpha\ell} = 0$ for $\alpha > \ell$ or $\alpha < \ell - n$. This also implies that the $\mu_{\alpha\ell}$ form a sparse matrix. Let M_k be the $(k+n+1) \times (k+n+1)$ matrix defined by

$$[M_k]_{\ell m} = \sum_{\alpha=0}^k a_{\ell-\alpha} a_{m-\alpha}^* \mu_{\alpha\ell} \mu_{\alpha m}. \quad (G6)$$

Eq. (F2) implies that $\xi_k = \lambda_{\max}(M_k)$, or equivalently, $\xi_k = s_{\max}^2(V_k)$, where $s_{\max}(\cdot)$ denotes the largest singular value and V_k is a $(k+n+1) \times (k+1)$ sparse matrix defined by

$$[V_k]_{\ell\alpha} = a_{\ell-\alpha} \mu_{\alpha\ell}. \quad (G7)$$

Similarly, for a general N -qubit state $|\psi\rangle = a_{i_1 i_2 \dots i_N} |i_1 i_2 \dots i_N\rangle$, we obtain the $(k+1)^N \times (k+1)^N$ matrix M_k

$$[M_k]_{\ell_1 \dots \ell_N; m_1 \dots m_N} = \sum_{\alpha_1, \dots, \alpha_N=0}^{k-1} a_{\ell_1-\alpha_1, \dots, \ell_N-\alpha_N} a_{m_1-\alpha_1, \dots, m_N-\alpha_N}^* \mu_{\alpha_1 \ell_1} \mu_{\alpha_1 m_1} \dots \mu_{\alpha_N \ell_N} \mu_{\alpha_N m_N}, \quad (G8)$$

where

$$\mu_{\alpha\ell} = \begin{cases} \sqrt{\binom{k-1}{\alpha} / \binom{k}{\alpha}} = \sqrt{\frac{k-\alpha}{k}} & \ell = \alpha, \\ \sqrt{\binom{k-1}{\alpha} / \binom{k}{\alpha+1}} = \sqrt{\frac{\alpha+1}{k}} & \ell = \alpha+1, \\ 0 & \text{others.} \end{cases} \quad (G9)$$

Then ξ_k defined by Eq. (F3) is given by $\xi_k = \lambda_{\max}(M_k)$, or equivalently, $\xi_k = s_{\max}^2(V_k)$, where $s_{\max}(\cdot)$ denotes the largest singular value and V_k is a $(k+1)^N \times k^N$ sparse matrix defined by

$$[V_k]_{\ell_1 \dots \ell_N; \alpha_1 \dots \alpha_N} = a_{\ell_1-\alpha_1, \dots, \ell_N-\alpha_N} \mu_{\alpha_1 \ell_1} \dots \mu_{\alpha_N \ell_N}. \quad (G10)$$

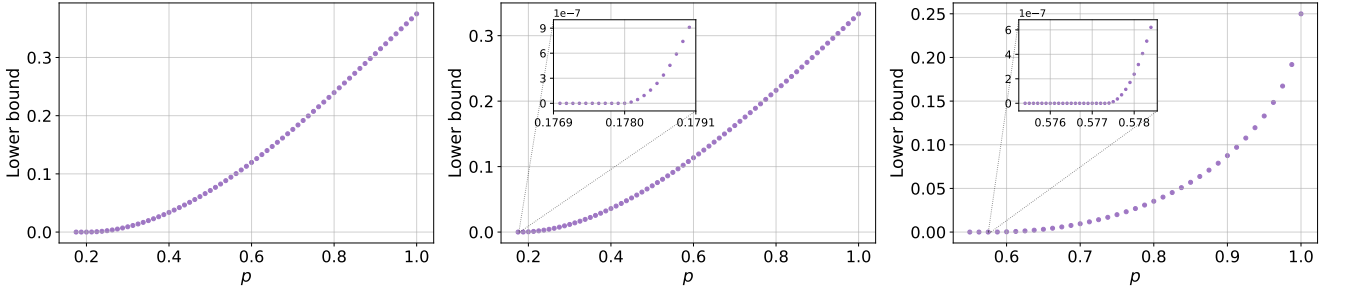


FIG. 6. (Left) Lower bounds for mixed states from the second level of the hierarchy (see Eq. (10) in the main text) for GHZ states mixed with white noise, $\rho(p) = p|\text{GHZ}\rangle\langle| + (1-p)\mathbb{1}/8$. (Middle) The estimate for W states with white noise, $\rho(p) = p|W\rangle\langle| + (1-p)\mathbb{1}/8$. These states are known to be fully separable for $p \leq 0.177$, entangled for $p > \sqrt{3}/(8+\sqrt{3}) \approx 0.1778$, but still separable for any bipartition until $p \leq 0.2095$. The inset shows the solution of the SDP for the W state with higher precision, i.e., smaller duality gap, in the parameter regime close to the border of separability. (Right) Lower bounds for mixed states from the second level of the hierarchy (see Eq. (10) in the main text) for Tao states mixed with white noise, $\rho(p) = p\tau + (1-p)\mathbb{1}/8$. The inset shows the solution of the SDP for the Tao state with higher precision, i.e., smaller duality gap, in the parameter regime close to the border of separability.

Appendix H: Application to operators

The first and third hierarchies can also be formulated for the separable numerical range of an operator. As an example, we consider an unextendible product basis (UPB) on a two qutrit-state, given by [33],

$$|\psi_0\rangle = \frac{1}{\sqrt{2}}|0\rangle(|0\rangle - |1\rangle), \quad (\text{H1})$$

$$|\psi_1\rangle = \frac{1}{\sqrt{2}}(|0\rangle - |1\rangle)|2\rangle, \quad (\text{H2})$$

$$|\psi_2\rangle = \frac{1}{\sqrt{2}}|2\rangle(|1\rangle - |2\rangle), \quad (\text{H3})$$

$$|\psi_3\rangle = \frac{1}{\sqrt{2}}(|1\rangle - |2\rangle)|0\rangle \text{ and} \quad (\text{H4})$$

$$|\psi_4\rangle = \frac{1}{3}(|0\rangle + |1\rangle + |2\rangle)(|0\rangle + |1\rangle + |2\rangle). \quad (\text{H5})$$

An UPB consists of a maximal set of orthogonal product states, meaning that no further product state orthogonal to all UPB states exists. Considering the projector on the UPB $P_{\text{UPB}} = \sum_{i=0}^4 |\psi_i\rangle\langle\psi_i|$, one finds then that the state $X_{\text{UPB}} \propto \mathbb{1} - P_{\text{UPB}}$ is entangled, since there exists no product state in its range. To construct an entanglement witness for this state one can consider $\mathcal{W}_{\text{UPB}} = P - \epsilon\mathbb{1}$, which should be positive on all product states [34, 35], leading to

$$\langle ab|W|ab\rangle = \langle ab|P|ab\rangle - \epsilon \geq 0 \Leftrightarrow \langle ab|P|ab\rangle \geq \epsilon \quad \forall|ab\rangle. \quad (\text{H6})$$

Thus, ideally one should choose $\epsilon = \min_{|ab\rangle} \langle ab|P|ab\rangle$, or equivalently $\delta = 1 - \epsilon = \max_{|ab\rangle} \langle ab|X_{\text{UPB}}|ab\rangle = M(X_{\text{UPB}})$. Formulating the first hierarchy we find therefore

$$\delta \leq \sqrt[k]{\lambda_{\max}(\Pi_k \otimes \Pi_k (X_{\text{UPB}})^{\otimes k} \Pi_k \otimes \Pi_k)} \quad (\text{H7})$$

while the third hierarchy in this case reads

$$\delta \leq \lambda_{\max} \left(\Pi_k \otimes \Pi_k X_{\text{UPB}} \otimes \mathbb{1}^{\otimes(k-1)} \Pi_k \otimes \Pi_k \right). \quad (\text{H8})$$

Appendix I: Lower bounds on the convex roof for mixed states

In order to test the estimation of the geometric measure for mixed states via Eq. (10) in the main text we implemented the SDP using the solver Mosek. For three qubits, the SDP requires a computation time of about thirty seconds on a standard laptop.

The results for the two examples discussed in the main text are displayed in Fig. 6. On the one hand, one finds that the SDP for the first level underestimates the amount of entanglement for highly entangled pure states. On the other hand, it provides a simple and very strong entanglement test for weakly entangled states. This is in line with the observations made in the main text as well as in Appendix C, where it was found that the hierarchies give good bounds for weakly entangled states.

While the noisy GHZ and W states have frequently been discussed, the three-qubit Tao state τ has been discovered only recently [47]. It is given by

$$\tau = \frac{1}{4} \begin{pmatrix} a & 0 & 0 & 0 & 0 & 0 & 0 & -c \\ 0 & b & 0 & 0 & 0 & 0 & ic & 0 \\ 0 & 0 & b & 0 & 0 & ic & 0 & 0 \\ 0 & 0 & 0 & a & -c & 0 & 0 & 0 \\ 0 & 0 & 0 & -c & b & 0 & 0 & 0 \\ 0 & 0 & -ic & 0 & 0 & a & 0 & 0 \\ 0 & -ic & 0 & 0 & 0 & 0 & a & 0 \\ -c & 0 & 0 & 0 & 0 & 0 & 0 & b \end{pmatrix}, \quad (\text{I1})$$

with $a = \cos^2(\vartheta)$, $b = \sin^2(\vartheta)$, $c = \cos(\vartheta) \sin(\vartheta)$ and $\vartheta = \arccos\left(\sqrt{1/2 + \sqrt{1/12}}\right)$. These states are biseparable for any fixed partition, an explicit decomposition is given in Ref. [47]. On the other hand, the state is not fully separable and hence entangled, actually the noisy state $\rho(p) = p\tau + (1-p)\mathbb{1}/8$ is provably entangled as long as $p \geq 0.5784$ and provably separable for $p \leq 0.5754$. This is a large noise robustness; actually, the state τ was found in Ref. [47] by an iteration of semidefinite programs looking for biseparable states with the highest robustness of entanglement. Using the first level of the hierarchy, one directly finds that the states $\rho(p)$ are entangled for $p \geq 0.5775$, demonstrating the usefulness of our approach to detect weakly entangled states.

[1] R. Horodecki, P. Horodecki, M. Horodecki, and K. Horodecki, Quantum entanglement, *Reviews of Modern Physics* **81**, 865 (2009).

[2] O. Ghne and G. Tth, Entanglement detection, *Physics Reports* **474**, 1–75 (2009).

[3] A. Shimony, Degree of entanglement, *Annals of the New York Academy of Sciences* **755**, 675 (1995).

[4] H. Barnum and N. Linden, Monotones and invariants for multi-particle quantum states, *Journal of Physics A: Mathematical and General* **34**, 6787 (2001).

[5] T.-C. Wei and P. M. Goldbart, Geometric measure of entanglement and applications to bipartite and multipartite quantum states, *Physical Review A* **68**, 042307 (2003).

[6] L. T. Weinbrenner and O. Ghne, Quantifying entanglement from the geometric perspective, *Europhysics Letters* **151**, 68001 (2025).

[7] S. Friedland, Tensors, entanglement, separability, and their complexity, [arXiv:2509.21639](https://arxiv.org/abs/2509.21639) (2025).

[8] W. Bruzda, S. Friedland, and K. yczkowski, Rank of a tensor and quantum entanglement, *Linear and Multilinear Algebra* **72**, 1796 (2024).

[9] A. W. Harrow and A. Montanaro, Testing product states, quantum Merlin-Arthur games and tensor optimization, *Journal of the ACM (JACM)* **60**, 1 (2013).

[10] A. C. Doherty, P. A. Parrilo, and F. M. Spedalieri, Complete family of separability criteria, *Physical Review A* **69**, 022308 (2004).

[11] X.-D. Yu, T. Simnacher, N. Wyderka, H. C. Nguyen, and O. Ghne, A complete hierarchy for the pure state marginal problem in quantum mechanics, *Nature communications* **12**, 1012 (2021).

[12] M. Navascus, S. Pironio, and A. Acn, A convergent hierarchy of semidefinite programs characterizing the set of quantum correlations, *New Journal of Physics* **10**, 073013 (2008).

[13] J. B. Lasserre, Global optimization with polynomials and the problem of moments, *SIAM Journal on optimization* **11**, 796 (2001).

[14] F. Mintert, M. Ku, and A. Buchleitner, Concurrence of mixed multipartite quantum states, *Physical Review Letters* **95**, 260502 (2005).

[15] R. Beausoleil, W. Munro, T. Spiller, and W. van Dam, *Tests of quantum information* (U.S. Patent 2006/0056631 A1, March 2006).

[16] S. Foulds, V. Kendon, and T. Spiller, The controlled SWAP test for determining quantum entanglement, *Quantum Science and Technology* **6**, 035002 (2021).

[17] H. A. Helfgott, Strategies for bounding the spectral norm of a tensor, MathOverflow (2021).

[18] S. Friedland, Upper bounds for the spectral norm of symmetric tensors (2021), [arXiv:2104.09363](https://arxiv.org/abs/2104.09363).

[19] R. Renner, Symmetry of large physical systems implies independence of subsystems, *Nature Physics* **3**, 645 (2007).

[20] C. M. Caves, C. A. Fuchs, and R. Schack, Unknown quantum states: the quantum de Finetti representation, *Journal of Mathematical Physics* **43**, 4537 (2002).

[21] M. Christandl, R. König, G. Mitchison, and R. Renner, One-and-a-half quantum de Finetti theorems, *Communications in Mathematical Physics* **273**, 473 (2007).

[22] M. Bourennane, M. Eibl, C. Kurtsiefer, S. Gaertner, H. Weinfurter, O. Gühne, P. Hyllus, D. Bruß, M. Lewenstein, and A. Sanpera, Experimental detection of multipartite entanglement using witness operators, *Physical Review Letters* **92**, 087902 (2004).

[23] J. Steinberg and O. Gühne, Finding maximal quantum resources, *Physical Review A* **110**, 062428 (2024).

[24] P. Masajada, A. Philip, and A. Streltsov, *Entcalc: Toolkit for calculating geometric entanglement in multipartite quantum systems* (2025), [arXiv:2512.10884](https://arxiv.org/abs/2512.10884).

[25] A. She and H. Yuen, Unitary Property Testing Lower Bounds by Polynomials, in *14th Innovations in Theoretical Computer Science Conference (ITCS 2023)*, Leibniz International Proceedings in Informatics (LIPIcs), Vol. 251, edited by Y. Tauman Kalai (Schloss Dagstuhl – Leibniz-Zentrum für Informatik, Dagstuhl, Germany, 2023) pp. 96:1–96:17.

[26] Z. P. Bradshaw, M. L. LaBorde, and M. M. Wilde, Cycle index polynomials and generalized quantum separability tests, *Proceedings of the Royal Society A* **479**, 20220733 (2023).

[27] X. Liu, J. Tura, and A. Rico, Measuring multipartite entanglement efficiently by testing symmetries (2025), [arXiv:2511.07537](https://arxiv.org/abs/2511.07537).

[28] X. Liu, J. Knörzer, Z. J. Wang, and J. Tura, Generalized concentratable entanglement via parallelized permutation tests, *Physical Review Research* **7**, L032022 (2025).

[29] A. Elben, R. Kueng, H.-Y. R. Huang, R. van Bijnen, C. Kokail, M. Dalmonte, P. Calabrese, B. Kraus, J. Preskill, P. Zoller, and B. Vermersch, Mixed-state entanglement from local randomized measurements, *Physical Review Letters* **125**, 200501 (2020).

[30] P. Cieśliński, S. Imai, J. Dziewior, O. Gühne, L. Knips, W. Laskowski, J. Meinecke, T. Paterek, and T. Vértesi, Analysing quantum systems with randomised measurements, *Physics Reports* **1095**, 1–48 (2024).

[31] A. Montanaro, Learning stabilizer states by Bell sampling, [arXiv:1707.04012](https://arxiv.org/abs/1707.04012) (2017).

[32] Z. Puchała, P. Gawron, J. A. Miszczak, L. Skowronek, M.-D. Choi, and K. Życzkowski, Product numerical range in a space with tensor product structure, *Linear Algebra and its Applications* **434**, 327–342 (2011).

[33] C. H. Bennett, D. P. DiVincenzo, T. Mor, P. W. Shor, J. A. Smolin, and B. M. Terhal, Unextendible product bases and bound entanglement, *Physical Review Letters* **82**, 5385 (1999).

[34] O. Gühne, P. Hyllus, D. Bruß, A. Ekert, M. Lewenstein, C. Macchiavello, and A. Sanpera, Experimental detection of entanglement via witness operators and local measurements, *Journal of Modern Optics* **50**, 1079 (2003).

[35] B. M. Terhal, A family of indecomposable positive linear maps based on entangled quantum states, *Linear Algebra and its Applications* **323**, 61 (2001).

[36] L. Gurvits, Classical deterministic complexity of Edmonds' problem and quantum entanglement, in *Proceedings of the thirty-fifth annual ACM symposium on Theory of computing* (2003) pp. 10–19.

[37] S. Gharibian, Strong NP-hardness of the quantum separability problem, *Quantum Information & Computation* **10** (2010).

[38] H. Kampermann, O. Gühne, C. Wilmott, and D. Bruß, Algorithm for characterizing stochastic local operations and classical communication classes of multiparticle entanglement, *Physical Review A* **86**, 032307 (2012).

[39] C. Ritz, C. Spee, and O. Gühne, Characterizing multipartite entanglement classes via higher-dimensional embeddings, *Journal of Physics A: Mathematical and Theoretical* **52**, 335302 (2019).

[40] O. Gühne, F. Bodoky, and M. Blaauboer, Multiparticle entanglement under the influence of decoherence, *Physical Review A* **78**, 060301 (2008).

[41] L. E. Buchholz, T. Moroder, and O. Gühne, Evaluating the geometric measure of multipartite entanglement, *Annalen der Physik* **528**, 278 (2016).

[42] G. Tóth, T. Moroder, and O. Gühne, Evaluating convex roof entanglement measures, *Physical Review Letters* **114**, 160501 (2015).

[43] F. Mintert, Entanglement measures as physical observables, *Applied Physics B* **89**, 493 (2007).

[44] R. Schack and C. M. Caves, Explicit product ensembles for separable quantum states, *Journal of Modern Optics* **47**, 387 (2000).

[45] W. Dür and J. I. Cirac, Classification of multiqubit mixed states: Separability and distillability properties, *Physical Review A* **61**, 042314 (2000).

[46] Z.-H. Chen, Z.-H. Ma, O. Gühne, and S. Severini, Estimating entanglement monotones with a generalization of the Wootters formula, *Physical Review Letters* **109**, 200503 (2012).

[47] T.-A. Ohst, X.-D. Yu, O. Gühne, and H. C. Nguyen, Certifying quantum separability with adaptive polytopes, *SciPost Phys.* **16**, 063 (2024).

[48] J. L. Beckey, N. Gigena, P. J. Coles, and M. Cerezo, Computable and operationally meaningful multipartite entanglement measures, *Physical Review Letters* **127**, 140501 (2021).

[49] L. Schatzki, G. Liu, M. Cerezo, and E. Chitambar, Hierarchy of multipartite correlations based on concentratable entanglement, *Physical Review Research* **6**, 023019 (2024).

[50] A. Neven, P. Mathonet, O. Gühne, and T. Bastin, Quantum fidelity of symmetric multipartite states, *Physical Review A* **94**, 052332 (2016).

[51] A. W. Harrow, The church of the symmetric subspace, [arXiv:1308.6595](https://arxiv.org/abs/1308.6595) (2013).

[52] S. Montangero, *Introduction to tensor network methods* (Springer, 2018).

- [53] S. Friedland and L.-H. Lim, Nuclear norm of higher-order tensors, *Mathematics of Computation* **87**, 1255 (2018).
- [54] G. Chartrand and P. Zhang, *A First Course in Graph Theory* (Dover Publications, Mineola, New York, 2012).
- [55] L. Hörmander, On a theorem of Grace, *Mathematica Scandinavica* **2**, 55 (1954).
- [56] R. Hübener, M. Kleinmann, T.-C. Wei, C. González-Guillén, and O. Gühne, Geometric measure of entanglement for symmetric states, *Physical Review A* **80**, 032324 (2009).
- [57] A. C. Doherty, P. A. Parrilo, and F. M. Spedalieri, Detecting multipartite entanglement, *Physical Review A* **71**, 032333 (2005).